atmosphere

Article

Effect of Heating Emissions on the Fractal Size Distribution of Atmospheric Particle Concentrations

Namkha Norbu [1], Xiaolei Sheng [1,*], Qiang Liu [1], Haihui Han [2] and Xin Zhang [3]

[1] Shaanxi Provincial Land Engineering Construction Group, Xi'an 710075, China; nkew1989@163.com (N.N.); qiangliu1988@163.com (Q.L.)
[2] Technology Innovation Center for Intelligent Remote Sensing Monitoring of Natural Resources in the Upper and Middle Reaches of the Yellow River, MNR, Xi'an 710054, China; hhaihui@mail.cgs.gov.cn
[3] School of Resources Engineering, Xi'an University of Architecture and Technology, Xi'an 710055, China; zhangxin17@xauat.edu.cn
* Correspondence: xiaoleis84@163.com

Abstract: Excessive particle concentrations during heating periods, which greatly affect people's physical and mental health and their normal lives, continue to be a concern. It is more practical to understand and analyze the relationship between the fractal dimension and particle size concentration distribution of atmospheric particulate matter before and after adjusting heating energy consumption types. The data discussed and analyzed in this paper were collected by monitoring stations and measured from 2016 to 2018 in Xi'an. The data include fractal dimension and particle size concentration changes in the atmospheric particulate matter before and after adjusting the heating energy consumption types. The results indicate that adjusting the heating energy consumption types has a significant impact on particulate matter. The average concentration of $PM_{2.5}$ decreased by 26.4 $\mu g/m^3$. The average concentration of PM_{10} decreased by 31.8 $\mu g/m^3$. At the same time, the different particle sizes showed a downward trend. The particles ranging from 0.265 to 0.475 μm demonstrated the maximum decrease, which was 8.80%. The heating period in Xi'an mainly involves particles ranging from 0 to 0.475 μm. The fractal dimensions of the atmospheric particulate matter before and after adjusting the heating energy consumption types were 4.809 and 3.397, respectively. After adjusting the heating energy consumption types, the fractal dimension decreased by 1.412. At that time, the proportions of particle sizes that were less than 1.0 μm, 2.0 μm, and 2.5 μm decreased by 1.467%, 0.604%, and 0.424%, respectively. This paper provides new methods and a reference value for the distribution and effective control of atmospheric particulate matter by adjusting heating energy consumption types.

Keywords: adjusting heating energy; emissions; particles; application of fractals; fractal dimension

check for updates

Citation: Norbu, N.; Sheng, X.; Liu, Q.; Han, H.; Zhang, X. Effect of Heating Emissions on the Fractal Size Distribution of Atmospheric Particle Concentrations. *Atmosphere* **2024**, *15*, 95. https://doi.org/10.3390/atmos15010095

Academic Editors: Adrianos Retalis, Vasiliki Assimakopoulos and Kyriaki-Maria Fameli

Received: 27 November 2023
Revised: 26 December 2023
Accepted: 9 January 2024
Published: 11 January 2024

1. Introduction

The frequent occurrence of a high concentration of pollutants during the heating season has always been a topic of concern [1]. Related studies have shown that, in recent years [2], the concentration of pollutants exceeding the standard during the heating season in China has been increasing year by year. Cities such as Shijiazhuang and Xi'an are currently two of the major cities in China where smog occurs frequently [2,3]. Living in this environment for a long time can cause varying degrees of harm to the human body [4]. Therefore, it is important to effectively control the concentration of pollutants during the heating season.

Various countries around the world have adopted relevant policies and methods to control the concentration of pollutants in the environment [5–8]. The World Health Organization's air quality guidelines provide mid-term goals, with the targets for levels 1 to 4 of $PM_{2.5}$ being 75, 50, 37.5, and 25 $\mu g/m^3$. The targets for levels 1 to 4 of PM_{10} are 150, 100, 75, and 50 $\mu g/m^3$ [5]. Other countries have also formulated relevant standards based on their own situations [6,7]. China has formulated the "Environmental Air Quality Standard" based on its current development situation [8], outlining a first-level standard of 35 μg/m^3 for the daily average concentration limit of $PM_{2.5}$, with a secondary standard of 75 μg/m^3. The first-level standard for the daily average concentration limit of PM_{10} is 50 μg/m^3, with a secondary standard of 150 μg/m^3. The first-level standard and the second-level standard represent good air quality and poor air quality, respectively. The first-level standard refers to strict pollutant limits [8]. It is often used when there is a need to ensure a sterile indoor environment or when there are extremely high control requirements for indoor particulate matter pollution concentrations, specifically in clean rooms, wards, dust-free workshops, production lines, etc. The second-level standard refers to relatively relaxed pollutant limits [8], which can meet people's daily needs without the need to achieve 100% indoor-particulate-matter-free conditions. Specifically, it applies to places such as residential buildings, shopping malls, schools, airports, and libraries. Of course, this standard can also be used to meet the control needs for the indoor environmental hygiene of different personnel according to their actual requirements.

In addition, with the formulation and implementation of relevant policies, scholars from various countries have also conducted relevant research on the concentrations of particulate matter in the atmosphere [9–13]. The main focus has been on the source and composition of particulate matter [9], the harm caused by particulate matter [10], the distribution differences of particulate matter [11], and the correlation between particulate matter and other pollutants [12,13]. In addition, some research has been conducted on the distribution of particulate matter during the heating season. Although some research results have been achieved in this area, there is still a lack of research on the differences in the quantity, concentration, and particle size distribution of atmospheric particulate matter under the adjustment of heating energy consumption. The main reason for this is that the distribution of particulate matter during the heating season is influenced by many factors, such as the combustion of fossil fuels, differences in heating temperature and duration, and subjective factors [14,15]. Adjustments to heating methods and energy use can directly or indirectly affect the distribution of particulate matter [16], thereby requiring continuous research on atmospheric particulate matter during the heating season. For example, the transition from radiation heating to underfloor heating results in a relatively more concentrated heating temperature and better heating efficiency [17], which does not cause significant local temperature differences but still has a significant impact on the distribution of small particles. The heating mode has changed from individual heating to centralized heating, reducing the particulate matter emissions generated by individual households for heating [18]. At the same time, it has also reduced energy waste caused by incomplete combustion. Centralized heating also maintains a specific heating temperature in households, and centralized combustion reduces energy consumption and pollutant emissions. In addition, the transition from fossil fuel combustion heating to new energy sources such as electricity and natural gas for heating has resulted in an overall reduction in particulate matter emissions at the source [19], thereby promoting continuous research on atmospheric particulate matter during the heating season.

Moreover, due to the significant impact of low outdoor temperatures during the heating season, there may also be differences in particulate matter in the environment [20]. Relevant studies suggest that particulate matter in the atmosphere exists in multiple forms [20,21], and during the heating season, the probability of coagulation with particulate matter produced by fossil fuels increases [22], resulting in certain differences in its related characteristics and motion trajectories compared to those during the non-heating season [20]. According to [23], there are significant differences in the morphology of particulate matter during the heating season compared to the non-heating season, and there are more significant differences when comparing this morphology to that of traditional spherical particles. This requires continuous research on the quantity and concentration distribution of particulate matter in the atmosphere. Fractal theory is widely used to describe the different forms and particle size distributions of particulate matter due to its advantages [24–26]. Currently, some studies in China have applied fractal theory to describe the morphology of particulate matter [27,28], especially its fractal dimension of size [22]. However, there are few reports on the fractal dimension of atmospheric particulate matter under conditions of heating energy adjustment and its relationship with the particle size distribution concentration under these conditions. In addition, there is relatively little research on the fractal dimension under conditions of heating energy adjustment in a typical city such as Xi'an in the northwest region.

Therefore, monitoring and measured data from 2016 to 2018 are discussed and analyzed in this paper. The fractal dimension of atmospheric particulate matter in Xi'an under the effect of heating energy adjustment and its relationship with the particle size distribution concentration under the effect of heating energy adjustment based on fractal theory are also discussed. This paper provides reference value for an in-depth understanding of the impact of heating methods and energy usage adjustments on the distribution of atmospheric particulate matter and a new evaluation method for effective control under the effect of energy adjustment during the heating season.

2. Methods

The heating season in Xi'an spans from 15 November of one year to 15 March of the following year [7]. The data were sourced from the weather forecast website (http://www.tianqihoubao.com, accessed on 12 August 2022) and the Weather Network website (http://www.tianqi.com, accessed on 12 August 2022) [29]. The daily average concentrations of various pollutants in Xi'an City from 31 January 2016 to 31 December 2018 were identified. Among them, the heating energy consumption types in Xi'an were related to the switch from coal to electricity and coal to gas in 2017 [30]. Before the adjustment of heating energy consumption types, from 2016 to 2017, traditional coal was the main source of heating energy, and new energy fuels were not used. With the implementation of policies, the heating energy consumption types from 2017 to 2018 were mainly electricity and natural gas, and measures for their transformation were increased to reduce the use of traditional coal. Therefore, it is critical to analyze the concentration of particulate matter before and after adjusting heating energy consumption types.

In order to make the data more representative, the locations for collecting particulate matter data were selected from five regional locations in the east, west, north, south, and center of Xi'an City to more accurately reflect the distribution of particulate matter after energy adjustment. Particle testing was conducted by using relevant instruments for collection. The GRIMM1.109 aerosol particle size spectrometer (GRIMM Aerosol Technology Co., Ltd, Ainring, Germany) was used to test the concentration of particulate matter, with a measurement range of 2,000,000 P/L and a repeatability of 5%, and it was supplied by Beijing Saak-Mar Environmental Instrument Ltd., Beijing, China. A Teste480 detector was used to measure temperature and humidity, with a temperature measurement range of -100~+400 °C and a measurement accuracy of $\pm$0.3 °C (~0.1% of the measured value), and it was supplied by Shanghai Baoxin Instrument Ltd., Shanghai, China. Humidity measurement range: 0~100% RH; measurement accuracy: $\pm$1.4% RH (~0.7% measurement value). To ensure the validity of the data, relevant standards for processing were used as a reference [31,32]. The testing period was 5 months during the heating season, with 3 groups tested at each location every month. The 5th, 15th, and 25th of each month were selected for testing, and the test was repeated 2 times per group, totaling 150 groups. Each group was tested for 10 min, and the average value from these 10 min was taken.

The particle distribution was determined using the Mandelbrot fractal theory model. The calculation is shown in Equation (1) [24,33,34]:

$$n(>x) = C \times x^{-D} \tag{1}$$

where $n(>x)$ is the number of particles larger than x; D is the fractal dimension; and C is the constant.

The calculation steps were taken from [34,35], where, first, the percentage of particles within different particle size ranges is calculated. Next, the percentage of quantities greater than a certain particle size is determined, and the values pertaining particle size and the percentage of quantities are plotted, followed by linear fitting. Finally, the fractal dimension D is obtained based on the slope, expressed as Formula (2) [24,34,35].

$$D = -k \tag{2}$$

Here, k is the slope of the straight line.

3. Results

3.1. Distribution of Pollutant Concentration under Adjustment of Heating Energy Consumption Types

The distribution of various pollutants before and after adjusting the heating energy consumption types during the heating period is shown in Figure 1.

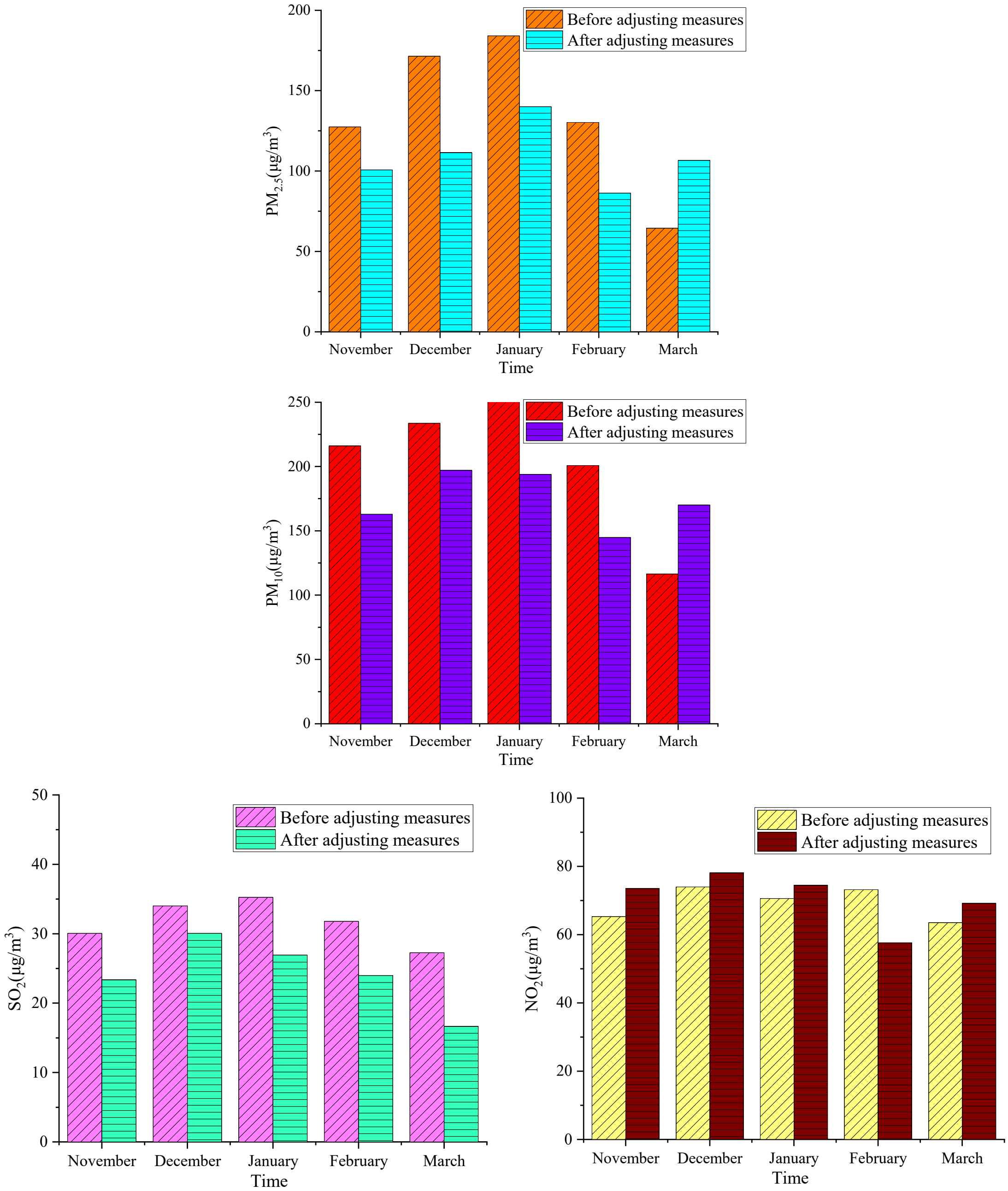

Figure 1. *Cont.*

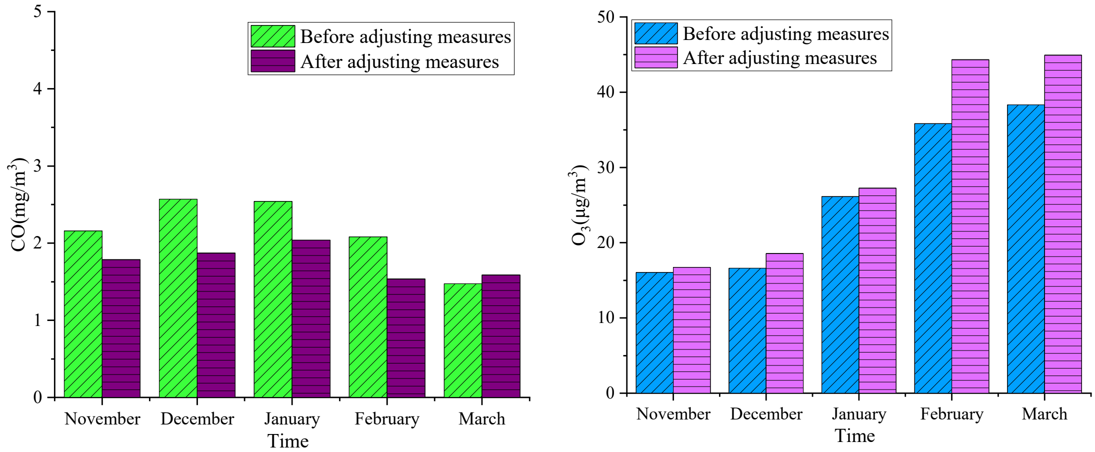

Figure 1. Distribution changes for various pollutants.

From Figure 1, it can be seen that the concentrations of various pollutants show different trends over time before and after adjusting the heating energy consumption types. Except for O_3, the other five pollutants show the highest concentrations in January and December and the lowest concentrations in November and March. O_3 shows the highest concentration in March and February and the lowest concentration in December and November. The maximum difference in the concentration of $PM_{2.5}$ before and after adjusting the heating energy consumption types occurred in December, with a difference of 59.9 $\mu g/m^3$. The maximum difference in the concentration of PM_{10} occurred in January, with a difference of 67.2 $\mu g/m^3$. The maximum difference in the concentration of SO_2 occurred in January, with a difference of 8.32 $\mu g/m^3$. The maximum difference in the concentration of NO_2 occurred in February, with a difference of 15.5 $\mu g/m^3$. The maximum difference in the concentration of CO occurred in December, with a difference of 0.700 mg/m^3. The maximum difference in the concentration of O_3 occurred in February, with a difference of 8.5 $\mu g/m^3$.

The average concentrations of $PM_{2.5}$ before and after adjusting the heating energy consumption types during the heating period are 135.5 $\mu g/m^3$ and 109.1 $\mu g/m^3$. The average concentration decreased by 26.4 $\mu g/m^3$. The average concentrations of PM_{10} were 205.6 $\mu g/m^3$ and 173.8 $\mu g/m^3$, and the average concentration decreased by 31.8 $\mu g/m^3$. The average concentrations of SO_2 were 31.7 $\mu g/m^3$ and 24.2 $\mu g/m^3$, and the average concentration decreased by 7.5 $\mu g/m^3$. The average concentrations of NO_2 were 69.3 $\mu g/m^3$ and 70.6 $\mu g/m^3$, and the average concentration increased by 1.30 $\mu g/m^3$. The average concentrations of CO were 2.16 mg/m^3 and 1.76 mg/m^3, and the average concentration decreased by 0.40 mg/m^3. The average concentrations of O_3 were 26.6 $\mu g/m^3$ and 30.4 $\mu g/m^3$, and the average concentration increased by 3.8 $\mu g/m^3$. It can be seen that adjusting the heating energy consumption types has a significant impact on the concentration of particulate matter. This is because the combustion of a large amount of fossil fuels during the heating season produces a large amount of particulate matter, and the relatively low air pressure in winter is less conducive to pollutant diffusion, making particulate matter the primary pollutant during this period [36]. The substitution of heating energy reduces the generation of pollutants, resulting in a relatively high concentration of particulate matter.

However, with the implementation of coal-to-electricity and coal-to-gas conversion, the generation of pollutants has been reduced, resulting in a relatively large decrease in the concentration of particulate matter. In addition, the relevant literature indicates that the production of SO_2 is accompanied by coal combustion [37]. Therefore, reducing the use of coal will lead to a decrease in the concentration of SO_2 in the air. The concentration of CO will also decrease at the same time. It also can be seen that the concentrations of some harmful gases are relatively high; the concentrations of NO_2 and O_3 have especially increased. This is because in recent years, the number of vehicles has gradually increased, and the relevant literature shows that cars produce NO_2 during the emission process [38], while the emitted nitrogen oxides will generate ozone when irradiated by sunlight [39]. As a result, the concentrations of NO_2 and O_3 become relatively high [40]. In addition, the greenhouse effect causes damage to the ozone layer [41], in addition to local emissions and the long-distance transport of pollutants. The combination of the above factors has led to relatively high concentrations of NO_2 and O_3. This also needs further in-depth research.

During the 121 days of the heating period, the peak daily average concentration of $PM_{2.5}$ before adjusting the heating energy consumption types occurred on 5 January 2017, amounting to 490 μg/m^3. The peak daily average concentration of PM_{10} occurred on 5 January 2017, amounting to 591 μg/m^3. The peak daily average concentration of $PM_{2.5}$ after adjusting the heating energy consumption types occurred on 28 December 2017, amounting to 304 μg/m^3. The peak daily average concentration of PM_{10} occurred on 29 December 2017, amounting to 513 μg/m^3. Therefore, it can be seen that adjusting the heating energy consumption types has a significant impact on the concentration of particulate matter. The daily average concentration limit of $PM_{2.5}$ before adjusting the heating energy consumption types exceeded the second-level standard (75 μg/m^3) for 88 days, and the exceeding rate was 72.7%. The daily average concentration limit of PM_{10} exceeded the second-level standard (150 μg/m^3) for 80 days, with an exceeding rate of 66.1%. After adjusting the heating energy consumption types, the daily average concentration limit of $PM_{2.5}$ exceeded the second-level standard (75 μg/m^3) for 85 days, with an exceeding rate of 70.2%. The daily average concentration limit of PM_{10} exceeded the second-level standard (150 μg/m^3) for 65 days, with an exceeding rate of 53.7%. After adjusting the heating energy consumption types, the exceeding rate of $PM_{2.5}$ decreased by 2.5%, and the exceeding rate of PM_{10} decreased by 12.4%. It can be seen that the concentrations of $PM_{2.5}$ and PM_{10} in the atmosphere still seriously exceed the standard. Traditional coal was the main source of heating energy before adjusting heating energy consumption types, and new energy fuels were not used. Furthermore, with the implementation of policies, the main forms of heating energy were electricity and natural gas after adjusting heating energy consumption types, and measures for their transformation were increased to reduce the use of traditional coal. It can be seen that adjusting heating energy consumption types is conducive to reductions in and the emission of particulate matter, so it is necessary to increase the adjustment of heating energy consumption types during the heating season. This conclusion is consistent with the conclusions given in relevant papers [42], verifying the correctness of this paper. However, the pollutant concentrations in March after the adjustment are relatively high due to the impact of sand and dust in the spring. As a result, extreme weather has a more significant impact on air pollution; this result is consistent with the conclusions given in relevant papers [43], verifying the correctness of this paper. So, it is necessary to control or avoid the occurrence of extreme weather in order to create good air quality.

3.2. Distribution of Particulate Matter Concentrations during Typical Months under the Effect of the Adjustment of Heating Energy Consumption Types

The distribution of particulate matter concentrations during the typical months with the highest pollutant concentrations during the heating period (December and January) was analyzed. The proportions of particulate matter for different particle sizes before and after adjusting the heating energy consumption types are shown in Figure 2.

Figure 2 shows that there are differences in the proportions of particulate matter for different particle sizes before and after adjusting the heating energy consumption types, and the overall trend shows a downward trend. The particles of a size less than 0.265 μm show an increasing trend, with an increase of 7.03% compared to that before adjusting the heating energy consumption types. The particles ranging from 0.265 to 0.475 μm decreased the most, with a decrease of 8.80%. Meanwhile, the differences in other large particle sizes are relatively small. This is because the energy adjustment reduced the overall emissions of particulate matter, resulting in a decrease in the chances of the collision and condensation of particulate matter in the air and in the overall particulate matter concentration. However, small particles can float in the air due to their lighter weight, and they can do so in relatively high concentrations. They are also relatively affected by meteorological parameters. When affected by sand and dust, the content of small particles in the air is relatively high, and the literature results verify the correctness of this paper in this regard [43]. As a result, the relative proportion of particles less than 0.265 μm is relatively high. However, overall, this reduces the combustion of fossil fuels, and the concentration of particulate matter decreases compared to that existing before adjusting the heating energy consumption types [36]. From the figure, it also can be seen that the heating period in Xi'an mainly involves particles ranging from 0 to 0.475 μm, which is consistent with the conclusions presented in [44], confirming the correctness of this paper. Figure 3 shows the changes in the concentration of accumulated particulate matter within different particle size ranges.

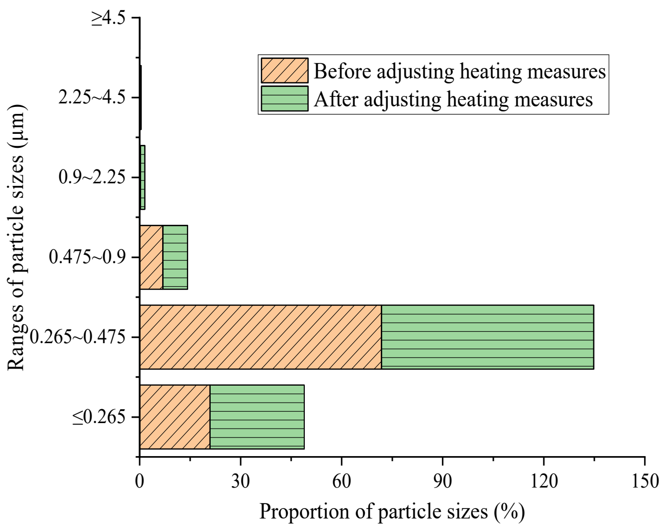

Figure 2. Proportions of particulate matter for different particle sizes in typical months.

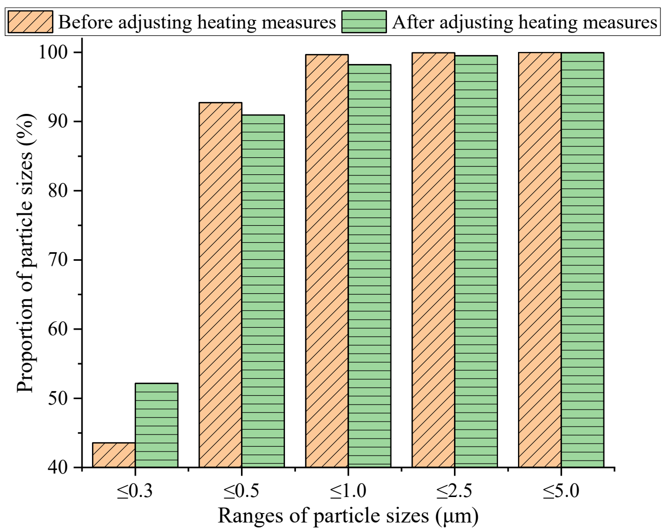

Figure 3. Proportions of accumulated particulate matter within different particle size ranges.

From Figure 3, it can be seen that after adjusting the heating energy consumption types, the proportion of accumulated particulate matter in different particle size ranges decreases overall. However, the proportion of particles less than 0.3 μm in size after adjusting the heating energy consumption types is higher than that before adjusting the heating energy consumption types. This is because small particles are greatly affected by the environment, and the overall concentration of particulate matter decreases after adjusting the heating energy consumption types; this also reduces interactions between small particles. In addition, the relevant literature provides burning conditions (effective or insufficient burning), and fuel may also lead to significant differences in the particle size distribution of particulate matter [45]. Secondary particulate matter mainly comes from the nucleation, condensation, or sublimation of organic or inorganic gases generated from the combustion of coal, biomass, and liquid fuels [46]. Therefore, the sources of small particles are more extensive and come in higher proportions. These small particles pose a more serious threat [47]. Understanding and analyzing the concentration distribution of small particle sizes before and after adjusting heating energy consumption types is more practical with respect to effectively controlling the concentration of particulate matter during the heating period.

3.3. Distribution of Fractal Dimensions of Typical Monthly Particles

Using Formulas (1) and (2), the relationship between the fractal dimensions and particle sizes of atmospheric particulate matter in typical months during the heating period in Xi'an is given, as shown in Figure 4.

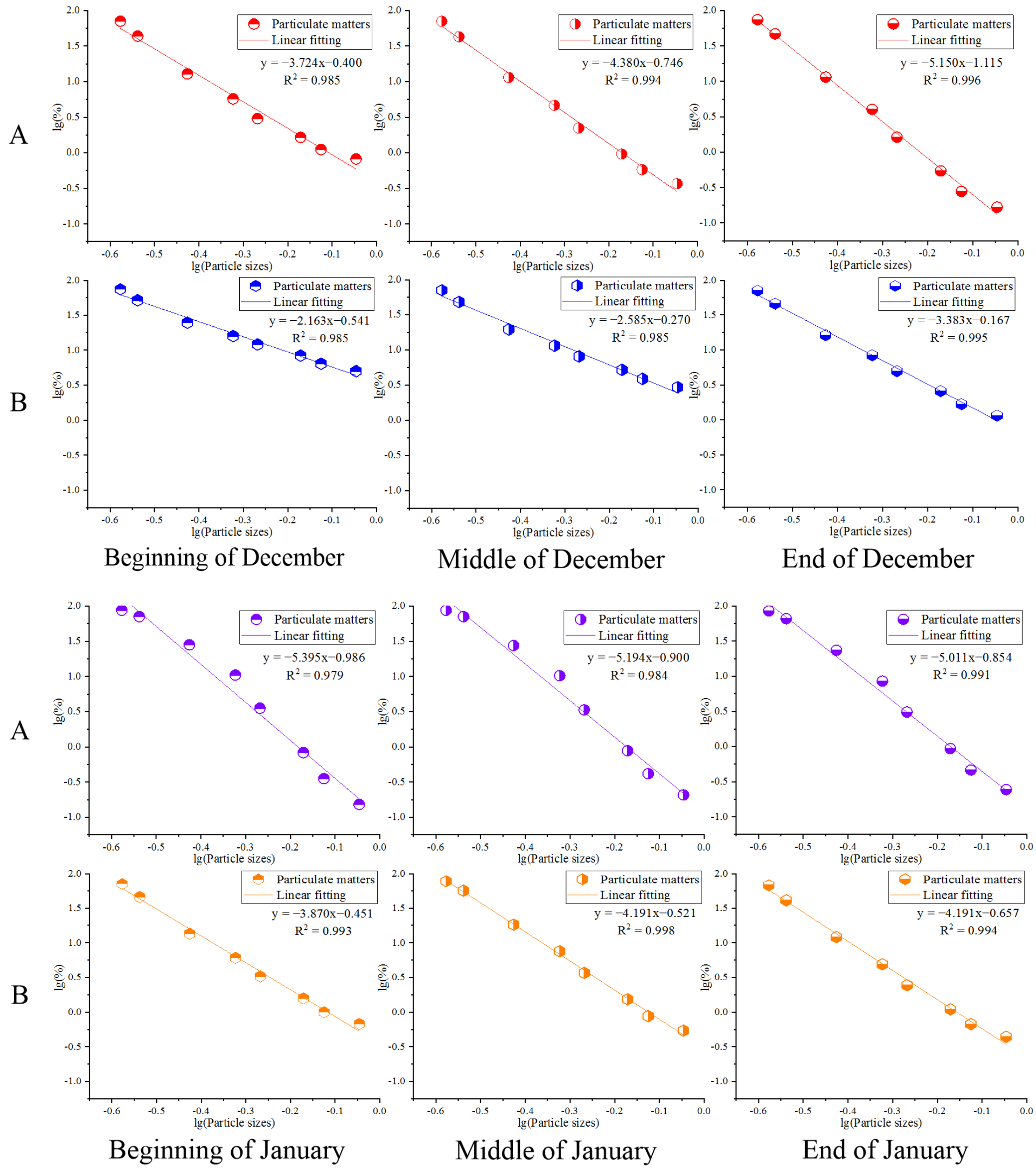

(**A**) Before adjusting heating measures. (**B**) After adjusting heating measures.

Figure 4. Fitting curve of fractal dimension of atmospheric particle size distribution.

From Figure 4, it can be seen that there is a negative correlation between the fractal dimension of particle size and the fitting curve of the particle size of atmospheric particulate matter in typical months during the heating period. This indicates that when particle size increases, the fractal dimension of particle size shows a decreasing trend and a good linear relationship. By using Formulas (1) and (2) again, the fractal dimension relationship with particle size before and after the overall heating energy adjustment is shown in Figure 5.

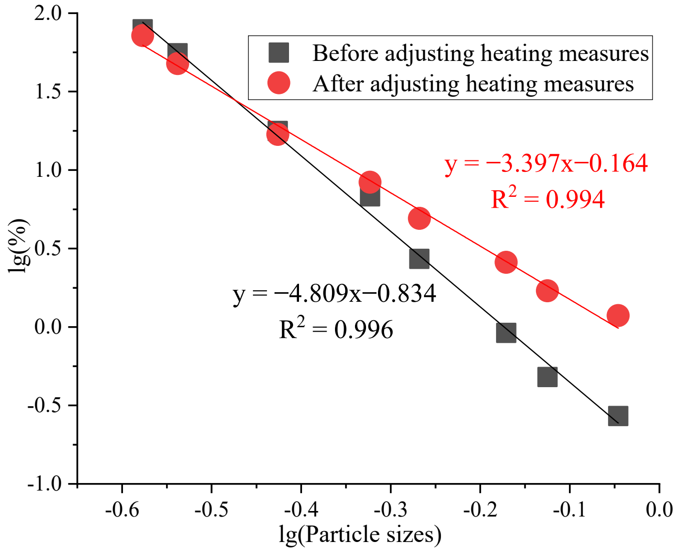

Figure 5. Fractal dimension of particle size before and after adjusting heating energy consumption types.

From Figure 5, it can be seen that the fractal dimensions of atmospheric particulate matter before and after adjusting the heating energy consumption types are 4.809 and 3.397, respectively. After adjusting the heating energy consumption types, the fractal dimension decreased by 1.412. The larger the fractal dimension value, the greater the proportion of fine particles. This indicates that the proportion of fine particles is relatively high before adjusting the heating energy consumption types, while the proportion of fine particles decreases significantly after adjusting the heating energy consumption types. Therefore, the fractal dimension can effectively reflect the uniformity of atmospheric particle composition.

Currently, the fractal dimensions given in the relevant research are mostly between 1 and 3 [48]. However, the fractal dimension values of atmospheric particulate matter during the heating period given in this paper are relatively large, indirectly indicating the differences and irregularities in the morphology of atmospheric particulate matter during the sampling period. This conclusion is consistent with the results presented in relevant papers [17,49,50], helping to verify the correctness of this paper. At the same time, this also indicates that the distribution of fine particulate matter is mainly in the atmosphere in and around Xi'an [6,44]. The results regarding the fractal dimension of the atmospheric fine particle size and its corresponding cumulative proportion of particulate matter before and after adjusting the heating energy consumption types are shown in Figure 6.

From Figure 6, it can be seen that the fractal dimension of the atmospheric particulate matter before adjusting the heating energy consumption types is 4.809. At this time, the proportions of particle sizes less than 1.0 µm, 2.0 µm, and 2.5 µm are 99.674%, 99.895%, and 99.934%, respectively. The fractal dimension of the atmospheric particulate matter after adjusting the heating energy consumption types is 3.397. At that time, the proportions of particle sizes less than 1.0 µm, 2.0 µm, and 2.5 µm are 98.207%, 99.291%, and 99.510%, respectively. After adjusting the heating energy consumption types, the proportions of particle sizes less than 1.0 µm, 2.0 µm, and 2.5 µm decreased by 1.467%, 0.604%, and 0.424%, respectively. Therefore, the fractal dimension can be used to characterize the relevant parameters of particulate matter. This study provides new methods and a reference value for the distribution and effective control of atmospheric particulate matter under the effect of the adjustment of heating energy consumption types.

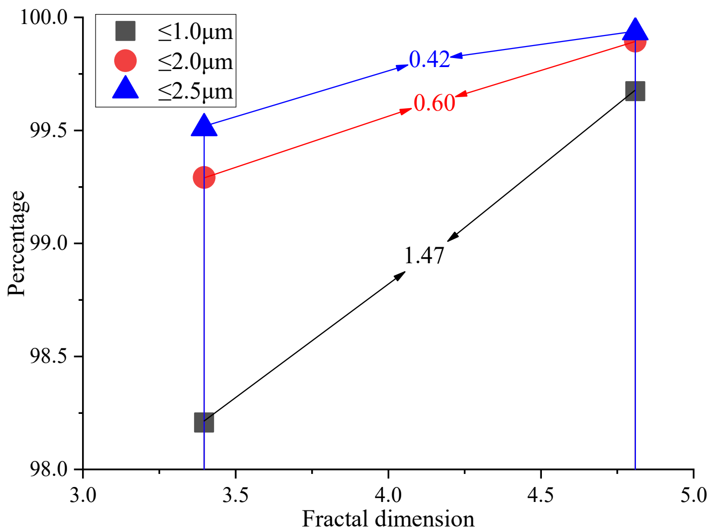

Figure 6. The fractal dimension of particulate matter and its corresponding cumulative proportion.

4. Conclusions

The data discussed and analyzed in this paper were collected by monitoring stations in Xi'an and measured from 2016 to 2018. The data include the fractal dimension and particle size concentration changes in atmospheric particulate matter before and after adjusting the heating energy consumption types. The conclusions are as follows:

1. After adjusting the heating energy consumption types, except for O_3, the other five pollutants showed the highest concentrations in January and December and the lowest concentrations in November and March. O_3 showed the highest concentration in March and February and the lowest concentration in December and November.
2. The average concentrations of $PM_{2.5}$ before and after adjusting the heating energy consumption types decreased by 26.4 $\mu g/m^3$. The average concentrations of PM_{10} decreased by 31.8% $\mu g/m^3$. The average concentrations of SO_2 decreased by 7.5 $\mu g/m^3$. The average concentrations of NO_2 increased by 1.30 $\mu g/m^3$. The average concentrations of CO decreased by 0.40 mg/m^3. The average concentrations of O_3 increased by 3.8 $\mu g/m^3$. Adjusting the heating energy consumption types has a significant impact on the concentration of particulate matter.
3. The different particle sizes showed a downward trend. The particles ranging from 0.265 to 0.475 μm decreased the most, with a decrease of 8.80%. The heating period in Xi'an mainly involves particles ranging from 0 to 0.475 μm.
4. The fractal dimensions of atmospheric particulate matter before and after adjusting the heating energy consumption types are 4.809 and 3.397. After adjusting the heating energy consumption types, the fractal dimension decreased by 1.412. This indicates that the proportion of fine particles decreases significantly after adjusting heating energy consumption types. At this time, the proportions of particles less than 1.0 μm, 2.0 μm, and 2.5 μm decreased by 1.467%, 0.604%, and 0.424%, respectively. This provides new methods and reference value for the distribution and effective control of atmospheric particulate matter under the effect of adjusting heating energy consumption types. In future research, the distribution of particle sizes in the environment can be determined by evaluating the size of the fractal dimension.

Author Contributions: Conceptualization, N.N.; methodology, X.S. and X.Z.; data curation, Q.L.; resources, X.Z.; writing—original draft preparation, N.N. and X.S.; writing—review and editing, X.S. and H.H. All authors have read and agreed to the published version of the manuscript.

Funding: This study was supported by project of Shaanxi Province Land Engineering Construction Group (No. DJNY2024-19) and National Science Foundation of Shaanxi Provence of China (Grant No. 2023-JC-QN-0359).

Institutional Review Board Statement: Not applicable.

Informed Consent Statement: Not applicable.

Data Availability Statement: Raw data are available upon reasonable request addressed to the corresponding author on reasonable request. The data is sourced from the weather forecast website (http://www.tianqihoubao.com, accessed on 12 August 2022), Weather Network (http://www.tianqi.com, accessed on 12 August 2022). The source of the data has been reflected in the paper, as well as in the methodology.

Conflicts of Interest: Authors Namkha Norbu, Xiaolei Sheng and Qiang Liu were employed by the company Shaanxi Provincial Land Engineering Construction Group, Xi'an, China. The remaining authors declare that the research was conducted in the absence of any commercial or financial relationships that could be construed as a potential conflict of interest.

References

1. Jeon, J.; Chen, Y.; Kim, H. Influences of meteorology on emission sources and physicochemical properties of particulate matter in Seoul, Korea during the heating period. *Atmos. Environ.* **2023**, *303*, 119733. [CrossRef]
2. Pang, N.; Gao, J.; Che, F.; Ma, T.; Liu, S.; Yang, Y.; Zhao, P.; Yuan, J.; Liu, J.; Xu, Z.; et al. Cause of PM2.5 pollution during the 2016–2017 heating season in Beijing, Tianjin, and Langfang, China. *J. Environ. Sci.* **2020**, *95*, 201–209. [CrossRef]
3. Wang, J.; Wang, S.; Xu, X.; Li, X.; He, P.; Qiao, Y.; Chen, Y. The diminishing effects of winter heating on air quality in northern China. *J. Environ. Manag.* **2023**, *325*, 116536. [CrossRef] [PubMed]
4. Kim, K.-H.; Kabir, E.; Kabir, S. A review on the human health impact of airborne particulate matter. *Environ. Int.* **2015**, *74*, 136–143. [CrossRef] [PubMed]
5. Tong, D.; Geng, G.; Jiang, K.; Cheng, J.; Zheng, Y.; Hong, C.; Yan, L.; Zhang, Y.; Chen, X.; Bo, Y.; et al. Energy and emission pathways towards PM2.5 air quality attainment in the Beijing-Tianjin-Hebei region by 2030. *Sci. Total Environ.* **2019**, *692*, 361–370. [CrossRef] [PubMed]
6. Järvi, L.; Kurppa, M.; Kuuluvainen, H.; Rönkkö, T.; Karttunen, S.; Balling, A.; Timonen, H.; Niemi, J.V.; Pirjola, L. Determinants of spatial variability of air pollutant concentrations in a street canyon network measured using a mobile laboratory and a drone. *Sci. Total Environ.* **2023**, *856*, 158974. [CrossRef] [PubMed]
7. Gao, C.; Zhang, F.; Fang, D.; Wang, Q.; Liu, M. Spatial characteristics of change trends of air pollutants in Chinese urban areas during 2016–2020: The impact of air pollution controls and the COVID-19 pandemic. *Atmos. Res.* **2022**, *283*, 106539. [CrossRef]
8. *GB3095-2012*; Ambient Air Quality Standards. China Environmental Science Press: Beijing, China, 2012.
9. Zhou, F.; Yang, J.; Wen, G.; Ma, Y.; Pan, H.; Geng, H.; Cao, J.; Zhao, M.; Xu, C. Estimating spatio-temporal variability of aerosol pollution in Yunnan Province, China. *Atmos. Pollut. Res.* **2022**, *13*, 101450. [CrossRef]
10. Kumar, P.; Singh, A.; Arora, T.; Singh, S.; Singh, R. Critical review on emerging health effects associated with the indoor air quality and its sustainable management. *Sci. Total Environ.* **2023**, *872*, 162163. [CrossRef]
11. Han, G.; Liu, M.; Li, X.; Zhang, Q. Sources and geochemical behaviors of rare earth elements in suspended particulate matter in a wet-dry tropical river. *Environ. Res.* **2023**, *218*, 115044. [CrossRef]
12. Wang, J.; Li, T.; Li, Z.; Fang, C. Study on the Spatial and Temporal Distribution Characteristics and Influencing Factors of Particulate Matter Pollution in Coal Production Cities in China. *Int. J. Environ. Res. Public Health* **2022**, *19*, 3228. [CrossRef] [PubMed]
13. Rajkumar, R.P. The Relationship between Ambient Fine Particulate Matter (PM2.5) Pollution and Depression: An Analysis of Data from 185 Countries. *Atmosphere* **2023**, *14*, 597. [CrossRef]
14. Mi, K.; Zhuang, R.; Zhang, Z.; Gao, J.; Pei, Q. Spatiotemporal characteristics of PM2.5 and its associated gas pollutants, a case in China. *Sustain. Cities Soc.* **2018**, *45*, 287–295. [CrossRef]
15. Desservettaz, M.; Pikridas, M.; Stavroulas, I.; Bougiatioti, A.; Liakakou, E.; Hatzianastassiou, N.; Sciare, J.; Mihalopoulos, N.; Bourtsoukidis, E. Emission of volatile organic compounds from residential biomass burning and their rapid chemical transformations. *Sci. Total Environ.* **2023**, *903*, 166592. [CrossRef] [PubMed]
16. Chicherin, S.; Anvari-Moghaddam, A. Adjusting heat demands using the operational data of district heating systems. *Energy* **2021**, *235*, 121368. [CrossRef]
17. Mazo, J.; Delgado, M.; Marin, J.M.; Zalba, B. Modeling a radiant floor system with Phase Change Material (PCM) integrated into a building simulation tool: Analysis of a case study of a floor heating system coupled to a heat pump. *Energy Build.* **2012**, *47*, 458–466. [CrossRef]
18. Rehman, H.U.; Hirvonen, J.; Sirén, K. Performance comparison between optimized design of a centralized and semi-decentralized community size solar district heating system. *Appl. Energy* **2018**, *229*, 1072–1094. [CrossRef]

19. Mohammad, N.; Mohamad Ishak, W.W.; Mustapa, S.I.; Ayodele, B.V. Natural gas as a key alternative energy source in sus-tainable renewable energy transition: A mini review. *Front. Energy Res.* **2021**, *9*, 625023. [CrossRef]
20. Liu, F.; Yu, T.; Leng, W.; Zhang, X. Distribution and Fractal Characteristics of Outdoor Particles in High-Rise Buildings Based on Fractal Theory. *Fractal Fract.* **2023**, *7*, 669. [CrossRef]
21. Davies, C. Particles in the atmosphere: A review. *J. Aerosol Sci.* **1987**, *18*, 469–477. [CrossRef]
22. Goudeli, E.; Eggersdorfer, M.L.; Pratsinis, S.E. Coagulation–Agglomeration of Fractal-like Particles: Structure and Self-Preserving Size Distribution. *Langmuir* **2015**, *31*, 1320–1327. [CrossRef] [PubMed]
23. Zhang, C.; Hu, Y.; Adams, M.D.; Liu, M.; Li, B.; Shi, T.; Li, C. Natural and human factors influencing urban particulate matter concentrations in central heating areas with long-term wearable monitoring devices. *Environ. Res.* **2022**, *215*, 114393. [CrossRef] [PubMed]
24. Mandelbrot, B.B. *The Fractal Geometry of Nature*; W.H. Freeman: San Francisco, CA, USA, 1982.
25. Mandelbrot, B. How Long Is the Coast of Britain? Statistical Self-Similarity and Fractional Dimension. *Science* **1967**, *156*, 636–638. [CrossRef] [PubMed]
26. Arasan, S.; Akbulut, S.; Hasiloglu, A.S. The relationship between the fractal dimension and shape properties of particles. *KSCE J. Civ. Eng.* **2011**, *15*, 1219–1225. [CrossRef]
27. Liu, Y.; Wang, H.; Yu, H. Numerical Model of Filtration Efficiency Based on Fractal Characteristics of Particulate Matter and Particle Filter. *Atmosphere* **2023**, *14*, 1689. [CrossRef]
28. Guzzo, P.L.; Ţălu, Ş.; Kulesza, S.; Bramowicz, M. A Fractal Description of Finely Ground Particles of Natural Quartz Using Particle Size and Image Analyses. *JOM* **2023**, *75*, 1333–1344. [CrossRef]
29. Zhang, X.; Sun, H.; Li, K.P.; Nie, X.X.; Fan, Y.S.; Wang, H.; Ma, J.Y. Comparison of the Application of Three Methods for the Determination of Outdoor PM2.5 Design Concentrations for Fresh Air Filtration Systems in China. *Int. J. Environ. Res. Public Health* **2022**, *19*, 16537. [CrossRef]
30. Zhang, H.L.; Hao, Q.L.; Li, G.L. Analysis of Pollution Concentration of Particulate Matter after Adjusting Heating Measures in Xi'an. *Build. Energy Environ.* **2020**, *39*, 54–57. (In Chinese)
31. *HJ633-2012*; Technical Regulation on Ambient Air Quality Index (On Trial). China Environmental Science Press: Beijing, China, 2012.
32. *HJ663-2013*; Technical Regulation for Ambient Air Quality Assessment (On Trial). China Environmental Science Press: Beijing, China, 2013.
33. Miao, L.C.; Qiu, Y.; Liu, S.Y. Fractal feature of coal mine waste discrete material. *J. Southeast Univ. Nat. Sci. Ed.* **2003**, *33*, 79–81. (In Chinese)
34. Jin, Y.; Wu, Y.; Li, H.; Zhao, M.; Pan, J. Definition of fractal topography to essential understanding of scale-invariance. *Sci. Rep.* **2017**, *7*, srep46672. [CrossRef]
35. Shao, L.Y.; Yang, S.S.; Zhao, H.Y.; Li, H. *Physicochemistry and Toxicology of Indoor Airborne Inhalable Particles*; China Meteorological Press: Beijing, China, 2012; pp. 180–203.
36. Zhu, C.L.; Li, X.Q.; Li, F.Y. Analysis on variation trends and related features of concentration of main air pollution in Xi'an. *Environ. Eng.* **2017**, *35*, 104–109. (In Chinese)
37. Wang, X.; Xu, J.; Ling, P.; An, X.; Han, H.; Chen, Y.; Jiang, L.; Wang, Y.; Su, S.; Hu, S.; et al. A study on the release characteristics and formation mechanism of SO_2 during co-combustion of sewage sludge and coal slime. *Fuel* **2023**, *333*, 126511. [CrossRef]
38. Hu, R.; Zhang, F.; Peng, Z.; Pei, Y. The NOx emission characteristics of gasoline vehicles during transient driving cycles. *Transp. Res. Part D Transp. Environ.* **2022**, *109*, 103386. [CrossRef]
39. Liu, T.; Sun, J.; Liu, B.H.; Li, M.; Deng, Y.B.; Jing, W.L.; Yang, J. Factors Influencing O_3 Concentration in Traffic and Urban Environments: A Case Study of Guangzhou City. *Int. J. Environ. Res. Public Health* **2022**, *19*, 12961. [CrossRef] [PubMed]
40. Adams, S.; Acheampong, A.O. Reducing carbon emissions: The role of renewable energy and democracy. *J. Clean. Prod.* **2019**, *240*, 118245. [CrossRef]
41. Neale, P.J.; Williamson, C.E.; Banaszak, A.T.; Häder, D.-P.; Hylander, S.; Ossola, R.; Rose, K.C.; Wängberg, S.; Zepp, R. The response of aquatic ecosystems to the interactive effects of stratospheric ozone depletion, UV radiation, and climate change. *Photochem. Photobiol. Sci.* **2023**, *22*, 1093–1127. [CrossRef]
42. Zhu, W.-K.; Wang, C.-Y.; Wang, L.-S.; Wu, X.-H.; Yue, Q. Analysis of energy-saving and environmental benefits from power structure adjustment in China: A comparative study from 2020 to 2060. *Sustain. Prod. Consum.* **2022**, *31*, 750–761. [CrossRef]
43. Xu, Y.L.; Xue, W.B.; Lei, Y.; Zhao, Y.; Cheng, S.Y.; Ren, Z.H.; Huang, Q. Impact of meteorological conditions on PM2.5 pollution in China during winter. *Atmosphere* **2018**, *9*, 429. [CrossRef]
44. Zhang, X.; Ma, J.; Wang, J.; Shi, H.; Guo, J.; Fan, Y.; Nie, X.; Guo, T.; Luo, X. Modifying the Fiber Structure and Filtration Performance of Polyester Materials Based on Two Different Preparation Methods. *Langmuir* **2023**, *39*, 3502–3511. [CrossRef]
45. Harni, S.D.; Saarikoski, S.; Kuula, J.; Helin, A.; Aurela, M.; Niemi, J.V.; Kousa, A.; Rönkkö, T.; Timonen, H. Effects of emission sources on the particle number size distribution of ambient air in the residential area. *Atmos. Environ.* **2023**, *293*, 119419. [CrossRef]
46. Rogula-Kozłowska, W. Size-segregated urban particulate matter: Mass closure, chemical composition, and primary and secondary matter content. *Air Qual. Atmos. Health* **2015**, *9*, 533–550. [CrossRef] [PubMed]
47. Bu, S.B.; Wang, Y.L.; Wang, H.Y.; Wang, F.; Tan, Y.F. Predicting spatio-temporal distribution of indoor multi-phase phthalates under the influence of particulate matter. *Built Environ.* **2022**, *221*, 109329. [CrossRef]

48. Lu, S.; Tang, H.M.; Zhang, Y.Q.; Gong, W.P.; Wang, L.Q. Effects of the particle-size distribution on the micro and macro be-havior of soils: Fractal dimension as an indicator of the spatial variability of a slip zone in a landslide. *Bull. Eng. Geol. Environ.* **2018**, *77*, 665–677. [CrossRef]
49. Valle, F.; Brucale, M.; Chiodini, S.; Bystrenova, E.; Albonetti, C. Nanoscale morphological analysis of soft matter aggregates with fractal dimension ranging from 1 to 3. *Micron* **2017**, *100*, 60–72. [CrossRef]
50. Yang, S.S.; Shao, L.Y.; Shen, R.R.; Li, W.J.; Zhang, G.L.; Tan, M.G. Fractal dimensions of size distribution of PM10 in Shanghai. *China Environ. Sci.* **2007**, *27*, 594–598. (In Chinese)